

# Measurements of large optical surfaces with a laser tracker

Tom L. Zobrist<sup>a</sup>, James H. Burge<sup>a,b</sup>, Warren B. Davison<sup>b</sup>, Hubert M. Martin<sup>b</sup>

<sup>a</sup>College of Optical Sciences, University of Arizona, Tucson, AZ 85721, USA

<sup>b</sup>Steward Observatory, University of Arizona, Tucson, AZ 85721, USA

## ABSTRACT

Surface measurements represent a significant part of the cost for manufacturing large aspheric optics. Both polished and rough ground surfaces must be measured with high precision and spatial resolution. We have developed a system that couples a commercial laser tracker with an advanced calibration technique and a system of external references. This system was built to measure the off-axis primary mirror segments for the Giant Magellan Telescope where it will guide loose abrasive grinding and initial polishing. The system is further expected to corroborate the optical interferometric tests of the completed mirrors, in several low-order aberrations. The design, analysis, calibration, and measured performance of this system will be presented.

**Keywords:** telescopes, optical fabrication, optical testing, laser metrology, aspheres

## 1. INTRODUCTION

The 25-m  $f/0.7$  primary mirror for the Giant Magellan Telescope (GMT), shown in Figure 1, is made of seven 8.4-m segments in a close packed array.<sup>1</sup> Each of the off-axis mirror segments has 14 mm of aspheric departure, which makes the fabrication and testing of the segments challenging.

The optical test for guiding the final figuring of the off-axis segments uses a set of mirrors and computer generated hologram (CGH) to provide a null corrector for full-aperture interferometry of the segment.<sup>2</sup> In order to corroborate the measurements from the principal optical test and ensure that the correct surface is manufactured, a set of independent verification tests were developed to provide measurement redundancy.<sup>3</sup> This paper discusses in detail one of these systems: a laser tracker measuring system that is used primarily to guide the loose abrasive grinding phase of fabrication, but is expected to provide accurate measurements of low order shape errors in the mirror segment to verify the principal test results as well.

A laser tracker is a commercial device that measures the position of a retroreflector in 3 dimensions by using a distance-measuring interferometer (DMI) and two angular encoders. It is sensitive to sub-micron displacements in the radial direction, and the encoder accuracy is on the order of 1 arcsecond. It is capable of measuring a mirror surface to sub-micron accuracy if the tracker is located at the center of curvature, so angular errors do not affect the surface measurement, and if rigid-body motion of the mirror and tracker can be controlled during the course of the measurement, typically several minutes to an hour. We have demonstrated this sort of accuracy in measurements of a 1.7 m off-axis mirror.<sup>4</sup> In order to achieve similar accuracy with a much larger mirror, we need to improve the accuracy of the angle measurements and add stability references that compensate for rigid-body motion and large-scale variations in refractive index.

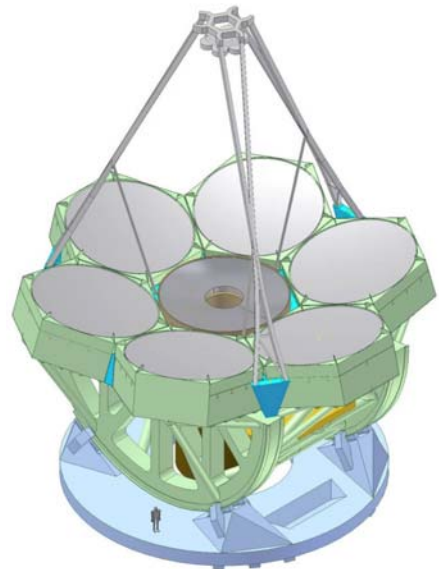


Figure 1. The 25 m  $f/0.7$  GMT primary mirror is made of 8.4-m diameter segments.

## 2. PRIOR TRACKER MEASUREMENTS AND LIMITATIONS

The use of the laser tracker for surface measurements builds on the experience from measuring the figure of the 1.7 m off-axis primary mirror of the New Solar Telescope (NST) at Big Bear Solar Observatory.<sup>4</sup> The NST mirror is very nearly a 1/5 scale model of the off-axis GMT segment, and served as a prototype for GMT fabrication and testing. The grinding and initial polishing of this surface was guided with the laser tracker exclusively. In the NST measurements, there was no attempt to improve the tracker's angular accuracy or to compensate for rigid-body motion or index variations. The tracker was mounted on the same structure that held the mirror, about 2 m above the mirror. This arrangement minimized relative motion between the mirror and the tracker, but placed the tracker far from the center of curvature ( $R = 7.7$  m), so the measurement was sensitive to angular errors. We found significant systematic errors in the tracker measurement that were reduced by averaging multiple measurements with the mirror rotated relative to the tracker. Figure 2 shows tracker data taken near the beginning of loose-abrasive grinding, with a measured error of  $14\ \mu\text{m}$  rms surface, and data measured near the end. The astigmatism seen in the early measurement was repeatable and was gradually reduced through figuring.

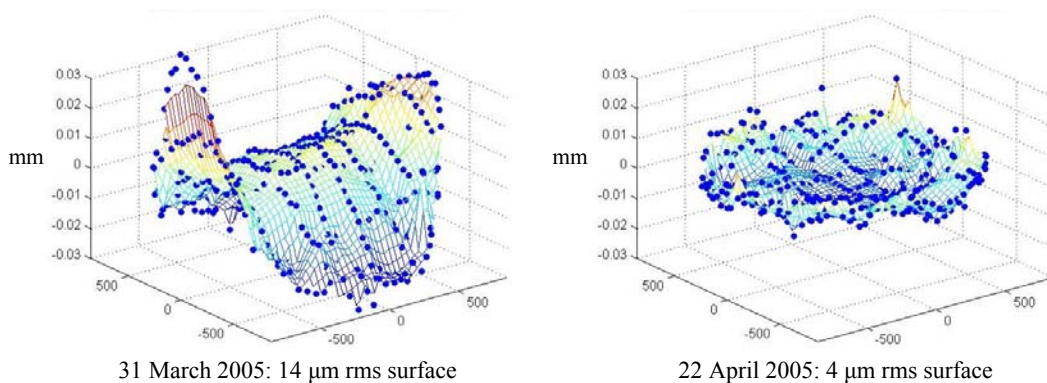


Figure 2: Laser tracker measurements of the NST mirror surface near the beginning of loose-abrasive grinding and near the end. The plots show the departure from the ideal off-axis paraboloid, with only piston, tip and tilt removed.

The purpose of the tracker measurements was to guide the figuring to an accuracy that would allow optical testing. Once it was polished, the mirror was measured using optical interferometry. The first optical measurement easily resolved fringes at  $633\ \text{nm}$  and matched the tracker measurement to about  $0.5\ \mu\text{m}$  rms. A comparison of interferometric and laser tracker measurements of NST is shown in Figure 3.

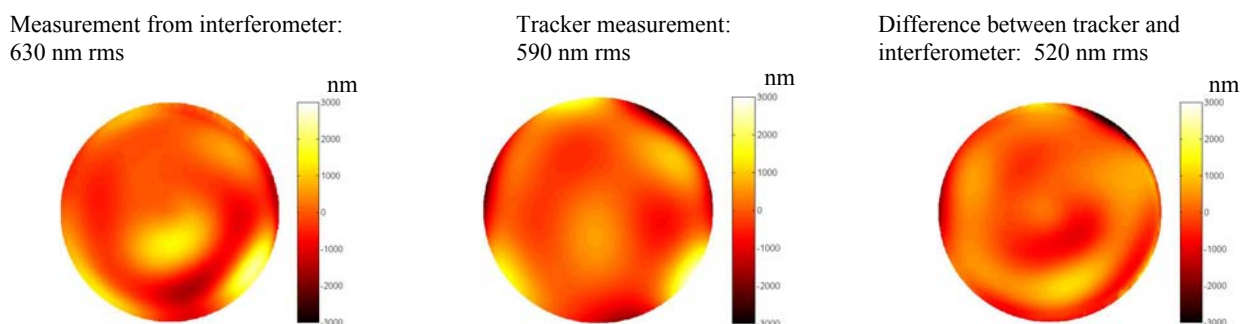


Figure 3: Comparison of one of the first optical measurements (image at left) with laser tracker data taken at the same time (center). The difference is shown on the right. The tracker map is a 6<sup>th</sup>-degree Zernike polynomial fit to the raw data. Focus, coma and astigmatism, which depend strongly on the alignment of the mirror in the optical test, were removed from all three maps.

### 3. LASER TRACKER PLUS

While we perform loose-abrasive grinding and initial polishing of the GMT segment, the optical surface is measured using a laser tracker mounted about 22 m above the mirror surface in the test tower. To measure the surface we move a sphere-mounted retroreflector (SMR) across the surface and measure its position. An SMR has a retroreflecting corner-cube mounted in a small steel sphere, with the corner of the cube at the center of the sphere. We improve the accuracy of this measurement by adding a set of external references to compensate for rigid-body motion and index variations, and by improving the calibration of the angular measurements. We call this enhanced system Laser Tracker Plus. The external references include four stand-alone DMIs, mounted on the same platform with the laser tracker, which monitor fixed retroreflectors at the edge of the mirror. They measure relative motion along the line of sight and changes in optical path length due to index variations. Some of the light from each of the DMIs is deflected to a position-sensing detector (PSD), which measures lateral displacement of the beam at each of the four positions. The PSD measurements can be used to compensate for relative motion perpendicular to the line of sight, including the effect of tilt of the laser tracker platform, and lateral motion of the beams due to large-scale index gradients.

This system, shown in Figure 4, fulfills two important functions:

- It does not require a specular surface, so we can use it to measure the rough surface to guide the generating and loose abrasive grinding operations.
- We can measure low order shape errors in the polished surface to  $< 1 \mu\text{m}$ , providing independent corroboration of these components of the mirror shape.

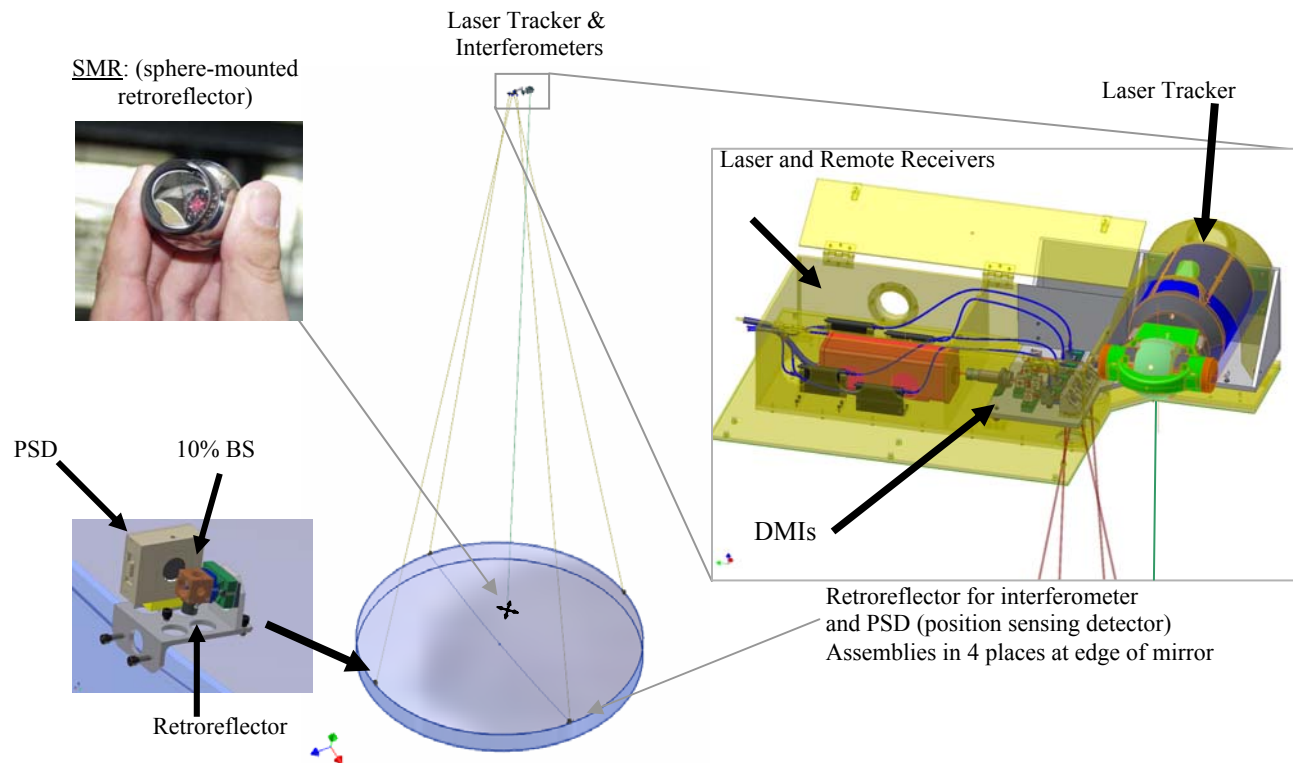


Figure 4. Conceptual drawing of the laser tracker set up for measuring the mirror surface. The laser tracker uses interferometry to measure distance to an SMR (sphere-mounted retroreflector). The tracker runs under servo control to follow the SMR as it is scanned across the surface, combining radial distance with the gimbal angles to make a three-dimensional measurement. Effects due to the combined motion of the air, mirror, and tracker are mitigated by separate real-time measurements of distance and lateral motion using four interferometer/position sensing detector systems.

#### 4. GEOMETRY & SENSITIVITY TO ERRORS

The laser tracker has excellent accuracy and sub-micron resolution for the line of sight distance, measured with its internal DMI. The angular measurements are accurate to 0.5-1 arcsecond after a standard calibration using the commercial software. For the GMT measurement, this leads to errors in lateral displacement of 50-100  $\mu\text{m}$ . Ideally, the tracker would be mounted at the center of curvature of the optic, which minimizes the sensitivity to angles. In practice, this point is not accessible for some optics, including convex optics and the GMT segment, whose center of curvature is 38 m above the segment and outside the Mirror Lab. The geometry for this system is shown in Figure 5. The angle  $\alpha$ , which is the deviation of the line of sight from the surface normal, is calculated approximately for a spherical mirror, assuming small angles:

$$\alpha \cong \arcsin\left(\frac{x}{h}\right) - \arcsin\left(\frac{x}{R}\right) \cong \frac{x}{R} \left(\frac{R-h}{h}\right). \quad (\text{Eq. 1})$$

The sensitivity of the measured distance  $r$  to position  $x$  on the mirror is  $\frac{dr}{dx} \cong \alpha \cong \frac{x}{R} \left(\frac{R-h}{h}\right)$ .

The GMT test with the tracker 22.3 m above the mirror has sensitivity of 74  $\mu\text{m}/\text{mm}$  at the outer edge of the mirror, with an average sensitivity to radial position of 52  $\mu\text{m}/\text{mm}$ .

The sensitivity of the surface measurements to angular error in the line of sight of the tracker is

$$\frac{dr}{d\theta} \cong \alpha \cdot h \cong \frac{x}{R} (R-h). \quad (\text{Eq. 2})$$

The GMT test has sensitivity to angle of 1.6  $\mu\text{m}/\mu\text{rad}$  or 7.9  $\mu\text{m}/\text{arcseconds}$  at the outer edge of the mirror, with an average sensitivity to angle of 5.6  $\mu\text{m}/\text{arcseconds}$ . This is likely to be a significant source of error in the measurement. When it is combined with increased relative motion of the mirror and tracker over the 22 m separation, we would anticipate an accuracy of 5-10  $\mu\text{m}$  rms without the enhancements of the Laser Tracker Plus system.

The measurement errors due to the tracker can be reduced by a combination of calibration for systematic errors and averaging for non-repeating errors and noise. Systematic errors in the tracker can be calibrated to the noise limit using a small spherical reference mirror for radial errors and an auxiliary laser tracker or DMI for angular errors. This is discussed in Section 5.

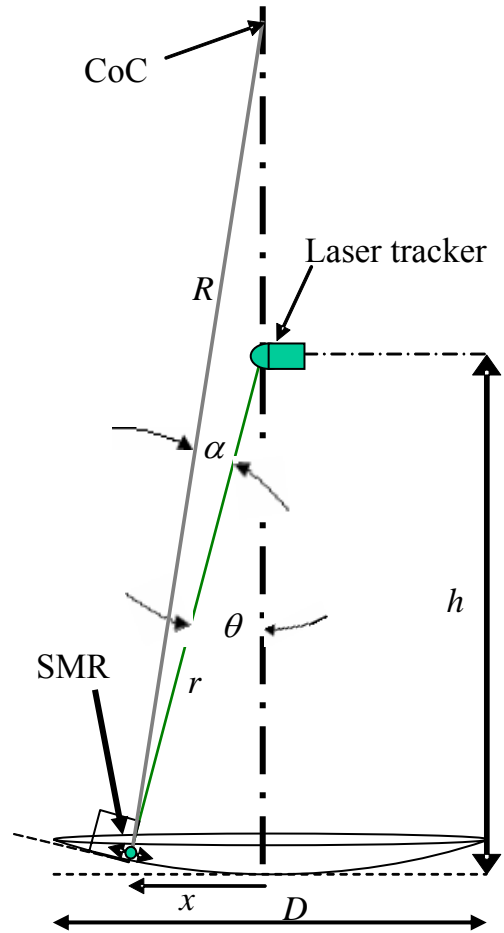


Figure 5: Geometry for the laser-tracker measurement of a mirror surface. By placing the laser tracker near the center of curvature, the measurements are made at near-normal incidence and the sensitivity to errors in the angles is minimized.

## 5. CALIBRATION CONCEPTS & RESULTS

To improve the accuracy of the commercial laser tracker, we devised a set of custom calibrations to measure repeatable intrinsic errors in the laser tracker. There are both radial and angular calibrations which determine the repeatable errors in the laser tracker's measurement of radius as a function of angle, and each angle as a function of angle.

### 5.1 Radial calibration

We calibrate the measurement of radial displacement by measuring a small reference sphere from its center of curvature. The measurement is insensitive to angular errors, allowing a determination of the repeatable portion of the radial error. A 150 mm diameter  $f/1.6$  spherical mirror was selected, covering a larger solid angle than the  $f/2.6$  cone that an 8.4 m mirror subtends from the tracker. Additionally, the size of the mirror allows it to be installed for *in situ* calibration of the laser tracker while it is mounted in the tower. The mechanics were designed to maintain submicron alignment of the test mirror to the laser tracker while the surface is being measured with a 0.5 inch SMR.

Thirty separate measurements of the test mirror were made. We fit 45 Zernike polynomials to each measurement. We calculated the mean and standard deviation  $\sigma$  of each Zernike coefficient, and used them to generate the plot in Figure 6. The curve represents the mean for each Zernike coefficient and the error bars represent the uncertainty given an average of any 5 of the 30 measurements. The tilt and power aberrations are due to displacement of the laser tracker and can be neglected. This leaves the 0 degree astigmatism term to be the largest outlier at 0.03  $\mu\text{m}$ . The operational goal for the Laser Tracker Plus system is 0.25  $\mu\text{m}$ , so any aberration less than 0.05  $\mu\text{m}$  is considered negligible. No correction for radial errors is required.

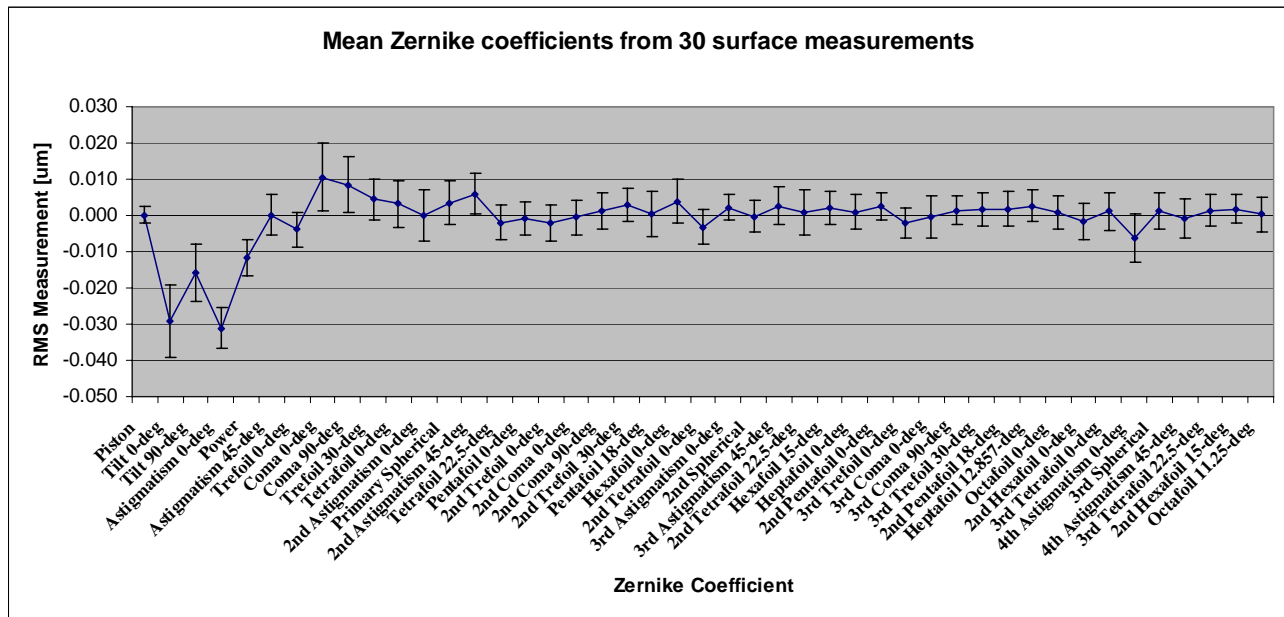


Figure 6: The RMS error introduced into each Zernike polynomial due to the radial errors in the laser tracker. The plot is based on 30 separate measurements of the surface, where the curve represents the mean for each Zernike coefficient and the error bars represent the uncertainty given an average of any 5 of the 30 measurements. The magnitude of the error bar is  $\pm \sigma/\sqrt{5}$ .

## 5.2 Angular calibration

The 3D accuracy of a laser tracker measurement is limited by the angular component of the measurement. The purpose of the angular calibration is to improve the angular accuracy by performing a custom calibration of one laser tracker with the use of a second laser tracker. The second laser tracker could be replaced by a stand-alone DMI.

The laser tracker in the tower is to be calibrated by a second laser tracker mounted at floor level, as illustrated by Figure 7. The tracker in the tower measures horizontal displacement of an SMR with its angular encoders, while the floor-mounted tracker measures the same displacement much more accurately with its DMI. The SMR has a narrow angle of acceptance, so a fixture has been designed that holds three 1.5 inch SMRs in direct contact along a straight line. The two outer balls are aimed upward toward the tracker to be calibrated, while the center ball is aimed horizontally toward the tracker at floor level. By measuring the locations of the two outer balls, the location of the center ball can be calculated.

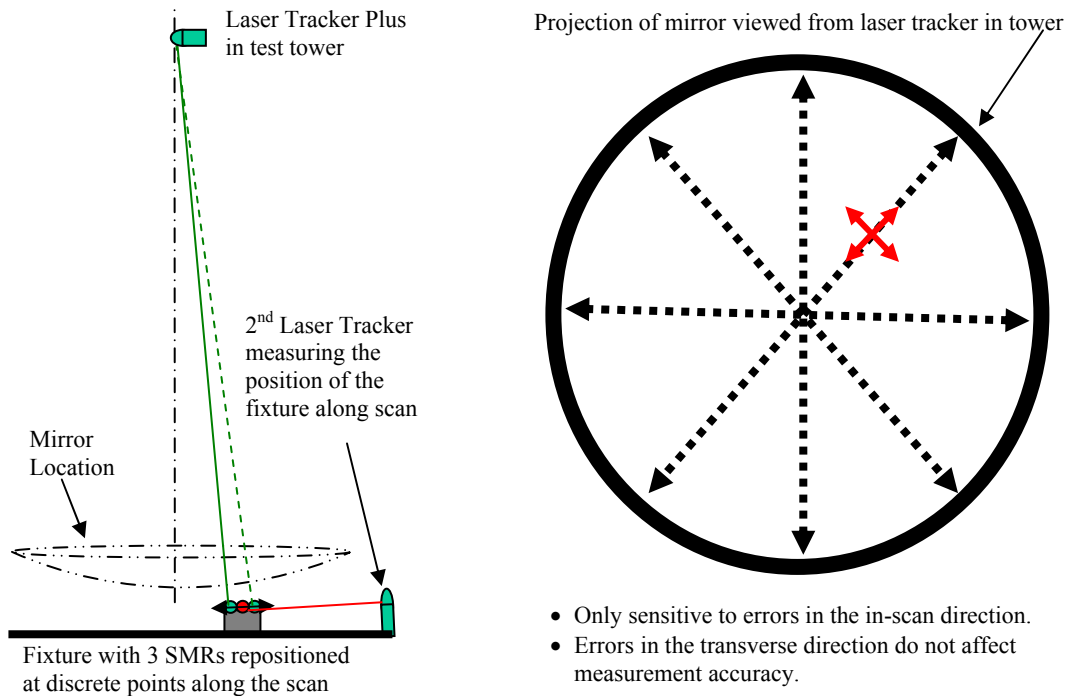


Figure 7: The diagram on the left shows the layout for the angular calibration. The laser tracker at floor measures the fixture location with small angular error compared to the tower tracker. The diagram on the right shows the pattern of multiple scans made to determine the discrepancy between the two trackers, which is used to determine a calibration correction for the angular errors.



## 6. TOP LEVEL PERFORMANCE

The design of the Laser Tracker Plus system was driven by a set of performance requirements and goals. It is difficult to project the ultimate accuracy of the system, so we established what we call minimum requirements, goals, and ambitious goals. The requirements and goals are related to the manufacturing specifications for the GMT segments. The segment specifications include tight tolerances on radius of curvature, off-axis distance and clocking angle, each of which corresponds to a particular low-order aberration or combination of aberrations. For example, an error in off-axis distance is equivalent to a combination of power, astigmatism, and coma in the surface. The segment specification also allows limited amounts of low-order aberrations like astigmatism that can be corrected at the telescope with the active mirror support and realignment of the segment. Table 1 lists the top-level requirements for each category, and some implied requirements.

Table 1. Requirements and goals for the Laser Tracker Plus system.

Top-level requirement	Implied requirements
<b>Minimum requirements</b>	
<ol style="list-style-type: none"> <li>1. Guide figuring to within capture range of principal optical test.</li> <li>2. Reduce geometry errors (<math>R</math>, off-axis distance, clocking) to levels that can be corrected by polishing (<math>\sim 10 \mu\text{m}</math> p-v surface).</li> </ol>	<ol style="list-style-type: none"> <li>1. Net accuracy of <math>2 \mu\text{m}</math> rms for first 10-15 Zernike polynomials.</li> <li>2. Measure distance from tracker to segment to 0.6 mm. <ul style="list-style-type: none"> <li>• equiv to <math>1 \mu\text{m}</math> rms defocus</li> </ul> </li> <li>3. Measure physical references at edge of segment to 1 mm. <ul style="list-style-type: none"> <li>• limits focus and astigmatism to <math>\sim 1 \mu\text{m}</math> rms</li> </ul> </li> </ol>
<b>Goals</b>	
<ol style="list-style-type: none"> <li>1. Verify that focus and astigmatism are small enough to be corrected within <math>\sim</math>half of 30 N rms force budget for active correction.</li> <li>2. Determine radius of curvature to 0.5 mm.</li> <li>3. Determine off-axis distance to 2 mm and clocking angle to 50 arcseconds.</li> </ol>	<ol style="list-style-type: none"> <li>1. Measure astigmatism to <math>1 \mu\text{m}</math> rms surface <ul style="list-style-type: none"> <li>• correctable with 12 N rms force</li> </ul> </li> <li>2. Measure defocus to <math>0.5 \mu\text{m}</math> rms. <ul style="list-style-type: none"> <li>• equiv to 0.3 mm radius error</li> <li>• correctable with 17 N rms force</li> </ul> </li> <li>3. Measure distance from tracker to segment to 0.3 mm.</li> <li>4. Measure physical references at edge of segment to 0.5 mm. <ul style="list-style-type: none"> <li>• equiv to 25 arcseconds clocking</li> </ul> </li> </ol>
<b>Ambitious goals</b>	
<ol style="list-style-type: none"> <li>1. Verify that focus, astigmatism <i>and coma</i> are small enough to be corrected within 30 N rms force budget.</li> <li>2. Determine radius of curvature to 0.3 mm.</li> <li>3. Determine off-axis distance to 1 mm.</li> </ol>	<ol style="list-style-type: none"> <li>1. Measure astigmatism to <math>0.5 \mu\text{m}</math> rms surface <ul style="list-style-type: none"> <li>• corresponds to 1 mm change in off-axis distance</li> <li>• correctable with 6 N rms force</li> </ul> </li> <li>2. Measure coma to <math>0.14 \mu\text{m}</math> rms surface <ul style="list-style-type: none"> <li>• correctable with 20 N rms force</li> </ul> </li> <li>3. Measure defocus to <math>0.3 \mu\text{m}</math> rms. <ul style="list-style-type: none"> <li>• equiv to 0.2 mm radius error</li> <li>• corresponds to 0.4 mm change in off-axis distance</li> <li>• correctable with 10 N rms force</li> </ul> </li> <li>4. Measure distance from tracker to segment to 0.2 mm.</li> </ol>

## 7. COMPONENTS OF LASER TRACKER PLUS

The full Laser Tracker Plus system combines three measurement subsystems and a fourth positioning system to accurately measure an optical surface. The three measurement subsystems are a commercial laser tracker, along with four distance measuring interferometers (DMI) and four position sensing detectors (PSD) which together form the external reference system, detailed in Figure 8. The positioning system moves the SMR between measurement locations across the mirror surface.

### 7.1 External reference system

The laser tracker and the DMIs are located up in the instrument package 22.3 m above the mirror, while the references which contain the PSDs and the retroreflectors for the DMIs are located on the mirror surface. The laser tracker and the DMIs are mounted on a common Invar optical bench to minimize relative motion between the two subsystems. The DMI system uses a single heterodyne HeNe laser, which is split into four beams. Each beam is directed into an interferometer then to a steering mirror that sends it to the retroreflector on the mirror. For each of the four reference arms, the retroreflector and PSD are mounted on a simple fixture that mounts kinematically on the edge of the mirror surface. It has adjustable nylon feet that allow radial positioning and fine tip/tilt adjustments. The fixture slides freely along the circumference of the mirror. Absolute position is not critical for these relative measurements, so the fixture is positioned to align to the beam from the DMI. A beamsplitter diverts 10% of the laser light to the PSD that measures the lateral displacement of the laser beam. The remainder of the light passes through the beamsplitter to the retroreflector that returns it to the interferometer. Fiber optic cables couple the light from the interferometers to remote receivers, where the optical signal is converted to an electronic signal and routed to a computer. The laser and remote receivers are mounted in a separate compartment from the DMI optics, and we ventilate the package to remove the heat generated by the electronics and the laser tracker.

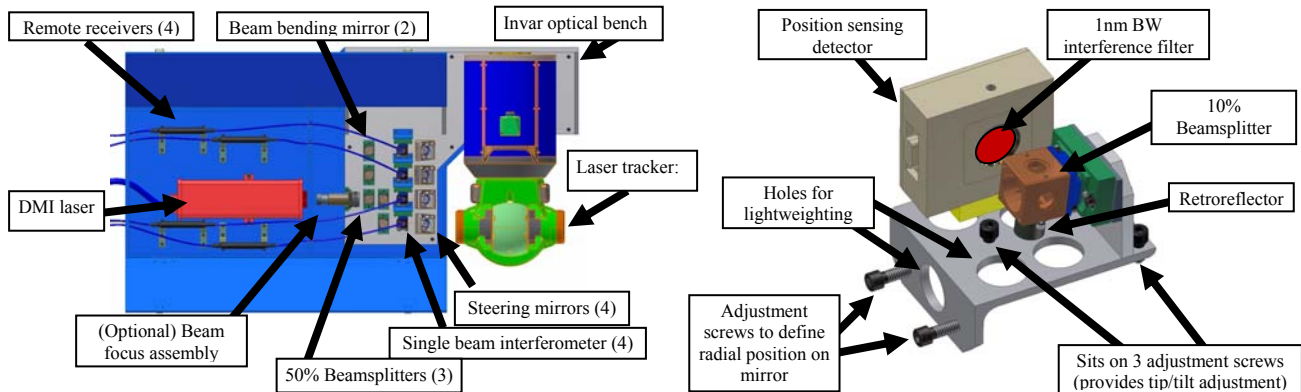


Figure 8: Detailed diagram of the Laser Tracker Plus instrument package mounted over the mirror, shown on the left, and one of the four references, shown on the right.

Each DMI measures the continuous relative change in optical path length along its reference arm. These changes may be caused by relative motion of the mirror and laser tracker or by index variations due to air turbulence or environmental drift, as illustrated in Figure 9. The four DMIs monitor the changes in path length along the four reference arms at the edge of the mirror. This information, coupled with the laser tracker measurement location with respect to the four reference locations, is used to estimate the radial error in the laser tracker measurements and compensate for it. The measurements of the reference arms must be made simultaneously with the laser tracker measurements.

The DMI laser output is  $600 \mu\text{W}$ , split evenly between the four reference arms. About  $22 \mu\text{W}$  of optical power is returned to the remote receivers, which have a minimum optical power requirement of  $2.2 \mu\text{W}$ , providing a radiometric safety factor of 10 for the DMI system.

The output of a position sensing detector (PSD) is a pair of analog voltage signals ( $\pm 10 \text{ V}$ ) to indicate the location of the centroid of the incident light on its detector face along each axis. This information can be used to



estimate the laser tracker's errors in lateral position and compensate for them. Again, coincident measurement times for the PSDs and laser tracker measurements are critical.

The PSDs are 10 mm x 10 mm dual-lateral position sensing modules used in conjunction with high-gain amplifiers, which provide a maximum gain of  $2.0 \times 10^7$  V/W. A 10% beamsplitter diverts  $0.87 \mu\text{W}$  of optical power to each of the PSDs. The amplifier at maximum gain will output 17 V, while the minimum requirement is 1 V, providing a radiometric safety factor of 17 for the PSD system.

The laser tracker's SMR may be anywhere on the mirror surface while the reference arms are at 4 fixed points at the edge. Correcting the tracker measurement involves some kind of average of the information from the 4 reference arms. The best recipe for averaging depends on the physical source of the error, which we generally do not know. A significant part of the error is likely to be rigid-body motion. We can fit a rigid-body motion (6 degrees of freedom) to the 4 radial displacements and 8 lateral displacements of the reference arms, using the redundant information to check for inconsistencies in the reference data. The correction to the tracker measurement would be obtained by taking the best-fit rigid-body displacement and evaluating it at the location of the SMR.

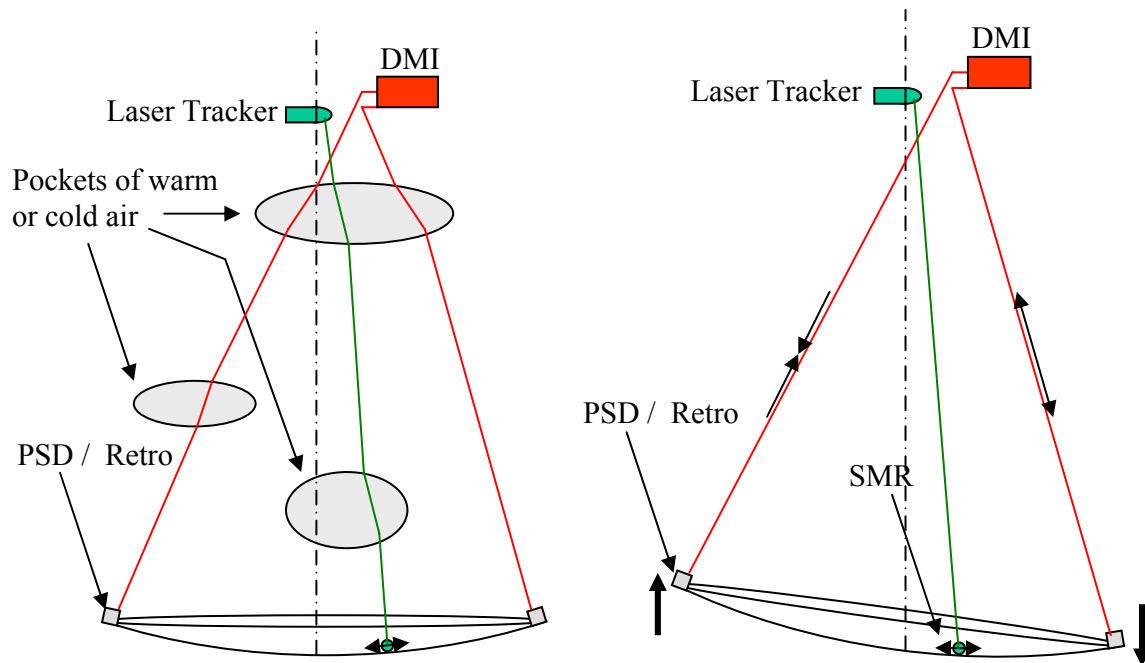


Figure 9: The external reference system can be used to compensate for refractive index variations as shown in the figure on the left, and for relative motion between the test instruments and the mirror surface as shown in the figure on the right.

Large-scale refractive index variations may look much like rigid-body motion and they can be corrected with the same recipe. Corrections for smaller-scale index variations may be optimized with a different recipe, for example a weighted average of the reference arms with the weighting depending on proximity. If the variations are on such a small scale that there is little correlation between the effects at the SMR and the nearest reference arm, there is no point in applying a correction, and the way to improve the measurement is to average over a longer time. We are investigating the spatial and temporal correlation of these effects. We will also experiment with different corrections and try to determine the best one(s) empirically.

## 7.2 SMR positioning system

A measurement with the Laser Tracker Plus system consists of something on the order of 100 samples, fairly uniformly distributed over the surface. The system includes a mechanism that moves the SMR over the surface of the mirror safely under computer control. This allows mirrors up to 8.4 m diameter to be measured without people being on the mirror or its support platform. It minimizes changing loads that would cause rigid-body motion.

The 1.5 inch SMR is carried by a puck made of plastic and rubber. The initial version of the puck uses a durable form of teflon that can slide across the glass surface without significant wear. In this version the SMR is separated from the glass by a thin layer of teflon, which maintains its thickness to a small fraction of a micron during the course of a measurement. We are using this version to measure the ground surface, but it poses a risk of scratching a polished surface. We are developing a new puck with three small flexible rubber air bearings that will be used on the polished surface. In this version the SMR rests on the glass while tracker data are recorded. Air pressure is applied to lift the puck and SMR a few mm above the surface while the air bearings remain nearly in contact with the glass. The puck slides to the next position with minimal force, and slowly lowers the SMR to the surface as the air bleeds out.

The puck is attached to four strings that control its position, as shown in Figure 10. The strings are controlled by motorized winches, two with position control and two holding constant tension. The winches and associated pulleys are mounted on steel beams about 3 m above floor level (slightly above the mirror surface) where they can be left permanently without interfering with traffic in the lab. Limit switches constrain the range of string positions so they cannot pull the SMR off the mirror or contact the four retroreflector/PSD assemblies at the edge of the mirror.

The SMR follows a pattern programmed into the control computer, pausing at each sample point long enough for the laser tracker and external reference system to make measurements before moving on to the next point. We aim to control the position to an accuracy of a few cm. The precise sample locations do not matter because the position is measured by the laser tracker.

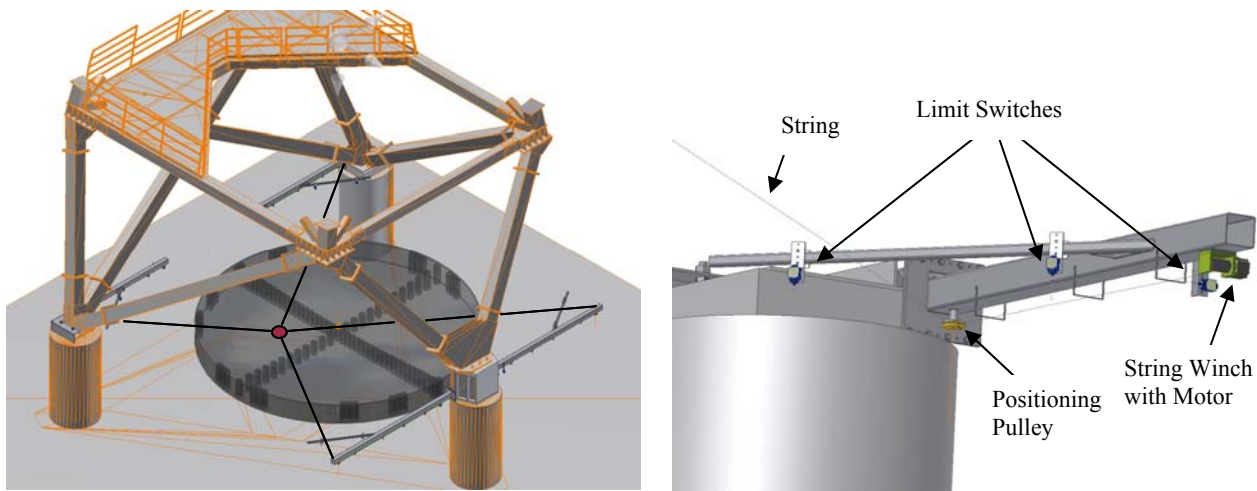


Figure 10: Diagram of the SMR positioning system at the base of the test tower. The gray disk represents the mirror under test, while the small circle at the intersection of the four strings is the location of the SMR puck. A close-up of one of the string control mechanism is shown on the right.

## 8. EXPERIMENTAL RESULTS

We were able to evaluate the accuracy of the Laser Tracker Plus system by measuring a finished 3.75 m spherical mirror. This mirror, shown in Figure 11, is part of the null corrector for the principal optical test of the GMT segment.<sup>5</sup> Its radius of curvature is 25.5 m. The mirror was mounted at the base of the 28 m test tower and the Laser Tracker Plus system was in its standard position near the top of the tower, about 22 m above the mirror. At the time of this measurement the SMR positioning system was not installed. We attached the SMR to a wooden wand and moved it manually from point to point on the mirror surface. This required that a person climb onto the mirror’s mounting platform to reach the wand and move the SMR. This caused up to 20  $\mu\text{m}$  of rigid-body motion of the mirror (as indicated by the reference DMIs) but it was largely elastic. For the results presented here, the SMR positioner climbed on the platform to reposition the SMR for each sample and climbed off before the data were recorded. We took 93 samples over a period of about 1.5 hours, averaging the laser tracker, DMIs and PSDs over 10 s for each sample.

We processed the laser tracker data by fitting a spherical surface. For each sample we applied the DMI correction by fitting a plane to the 4 DMI displacements (projected to the vertical direction), and evaluating the plane at the lateral position of the SMR (as measured by the laser tracker). We did not use the reference PSDs for this



Figure 11: Testing of the 3.75 m spherical mirror with the Laser Tracker Plus system. One of the references is visible in the foreground, with two of the three other visible in the background. An optician positions the SMR mounted at the end of a wooden wand for the next measurement.

measurement. Figure 12 shows the deviation from the best-fit sphere, before and after applying corrections based on the reference DMIs. The rms deviation is  $1.4\ \mu\text{m}$  with no DMI correction, and  $0.75\ \mu\text{m}$  after the DMI correction. An optical interferometer measurement was made at about the same time as the Laser Tracker Plus measurement. The optical data shows that the mirror surface has about  $50\ \text{nm}$  rms astigmatism (which will be corrected in operation, along with other low-order aberrations, by the adjustable support) and  $40\ \text{nm}$  rms in other figure error. The  $0.75\ \mu\text{m}$  deviation of the corrected tracker data reflects the accuracy of the Laser Tracker Plus system in this geometry.

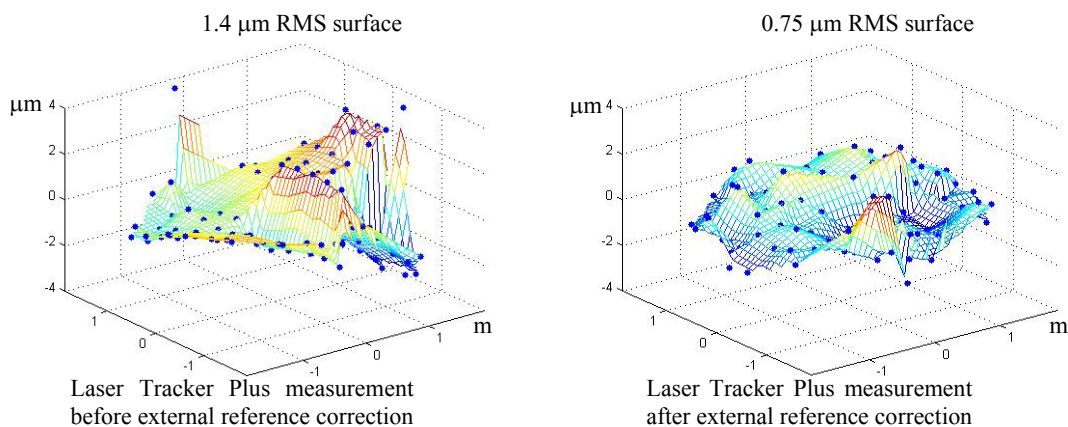


Figure 12: Measurements of a 3.75 m spherical mirror surface with the laser tracker only on the left, and the corrected plot after applying the data from the external reference system. The plots show the departure from the best-fit sphere, in microns, with only piston, tip and tilt removed.

Examination of the reference DMI data indicates rigid-body motion of 10  $\mu\text{m}$  peak-to-valley piston and 6  $\mu\text{m}$  p-v tilt during the measurement, and 0.8  $\mu\text{m}$  p-v deviation from the best-fit plane. This deviation may be due to temperature gradients or some kind of drift in the reference DMI system. If due to temperature gradients, it would imply 40 mK variations in the average temperature of one or more reference arms relative to the other arms, during the 1.5 hour measurement. We did not use the DMIs' deviation from a plane as part of the correction of laser tracker data.

The accuracy of 0.75  $\mu\text{m}$  rms is very encouraging for the first measurement with the Laser Tracker Plus system. When we measure the GMT segment, we anticipate some additional error because the laser tracker is farther from the center of curvature (causing greater sensitivity to angular error). With the addition of the SMR positioning system, however, we will be able to reduce rigid-body motion of the mirror during the measurement.

It is expected that the GMT mirror segment will be measured for the first time in July 2008. The front surface has been generated and loose-abrasive grinding has begun.<sup>6</sup> Once the majority of the generator marks have been removed and the surface is relatively smooth, the Laser Tracker Plus system will be used to measure the mirror's figure for guiding further loose-abrasive grinding.

## 9. CONCLUSION

A straightforward measurement of an optical surface with a commercial laser tracker at a distance of 22 m is expected to give an accuracy of 5-10  $\mu\text{m}$  rms per sample point. We have made two enhancements to the laser tracker measurements that should improve the accuracy by a significant factor. The first is the addition of stability references in the form of distance-measuring interferometers staring at fixed retroreflectors at the edge of the mirror. Part of each reference beam is also reflected to a position sensing detector that measures lateral displacement of the interferometer beam relative to the mirror. The second improvement is a calibration of the tracker in a geometry that matches the measurement geometry used for testing our mirrors.

With these improvements we expect the tracker measurement to be accurate to better than 2  $\mu\text{m}$  rms per sample point, and our goal is 0.5  $\mu\text{m}$  rms. The coefficients of low-order aberrations will be measured to better accuracy, limited by spatially correlated errors that are not removed by the stability references and calibration. We expect that the enhanced laser tracker system will provide independent measurements of radius of curvature and astigmatism, and potentially other low-order aberrations, at levels within the GMT requirements. When we make the transition from laser tracker measurements to optical testing, we expect the figure to be accurate enough that interference fringes are easily resolved.

## REFERENCES

- 
- [1] M. Johns, "The Giant Magellan Telescope (GMT)", in *Ground-based and Airborne Telescopes*, ed. L. M. Stepp, Proc. SPIE 6267 (2006).
  - [2] J. H. Burge, L. B. Kot, H. M. Martin, C. Zhao and R. Zehnder, "Design and analysis for interferometric testing of the GMT primary mirror segments", in *Optomechanical Technologies for Astronomy*, ed. E. Atad-Ettingui, J. Antebi and D. Lemke, Proc. SPIE 6273 (2006).
  - [3] J. H. Burge, L. B. Kot, H. M. Martin, C. Zhao and T. Zobrist, "Alternative surface measurements for GMT primary mirror segments", in *Optomechanical Technologies for Astronomy*, ed. E. Atad-Ettingui, J. Antebi and D. Lemke, Proc. SPIE 6273 (2006).
  - [4] H. M. Martin, J. H. Burge, S. D. Miller, B. K. Smith, R. Zehnder and C. Zhao, "Manufacture of a 1.7-m prototype of the GMT primary mirror segments", in *Optomechanical Technologies for Astronomy*, ed. E. Atad-Ettingui, J. Antebi and D. Lemke, Proc. SPIE 6273 (2006).
  - [5] J. H. Burge, W. Davison, C. Zhao and H. M. Martin, "Development of surface metrology for the Giant Magellan Telescope primary mirror", in *Advanced Optical and Mechanical Technologies in Telescopes and Instrumentation*, ed. E. Atad-Ettingui and D. Lemke, Proc. SPIE 7018 (2008).
  - [6] H. M. Martin, J. H. Burge, B. Cuerden, W. B. Davison, J. S. Kingsley, W. C. Kittrell, R. D. Lutz, S. M. Miller, C. Zhao and T. Zobrist, "Progress in manufacturing the first 8.4 m off-axis segment for the Giant Magellan Telescope", in *Advanced Optical and Mechanical Technologies in Telescopes and Instrumentation*, ed. E. Atad-Ettingui and D. Lemke, Proc. SPIE 7018 (2008).